Journal of Alloys and Compounds 514 (2012) 109–112

Contents lists available at SciVerse ScienceDirect

Journal of Alloys and Compounds

journal homepage: www.elsevier.com/locate/jallcom

# Synthesis and spectroscopic properties of $Er^{3+}$-doped $CaF_2$ nanocrystals in transparent oxyfluoride tellurite glass–ceramics

Zhao-xia Hou*, Zhao-lu Xue, Shao-hong Wang

*Key Laboratory of Advanced Materials Technology of Liaoning Province, Shengyang University, Shengyang 110044, China*

ARTICLE INFO

*Article history:*
Received 4 October 2011
Received in revised form 31 October 2011
Accepted 2 November 2011
Available online 11 November 2011

*Keywords:*
Glass–ceramics
Optical materials
Crystal structure
Luminescence
$Er^{3+}$ ions

ABSTRACT

Transparent glass–ceramics in $TeO_2$–$SiO_2$–$AlF_3$–CaO–NaF–$ErF_3$ system were prepared. Effect of heat-treatment schedules on crystallization behavior and microstructure were analyzed by differential scanning caborimetry, X-ray diffraction, infrared spectrum and scanning electron microscopy. The sole $CaF_2$ nanocrystal phase was confirmed, grains were spherical and distributed uniformly. Te and Si atoms existed in [$TeO_3$] and [$SiO_4$] forms. The full width at half maximum at 1533 nm emission increased from 39.16 nm to 43.37 nm after crystallization. $Er^{3+}$ ions were incorporated into $CaF_2$ nanocrystals with low phonon energies. The transmittance of glass–ceramics reached 78% at 780 nm and 90% at 1017 nm.



## 1. Introduction

$Er^{3+}$-doped glass and glass–ceramics are playing important role as lasers and optical amplifiers [1–4]. Oxyfluoride tellurite glass–ceramics is an ideal optical matrix material, it also has some advantages, such as low phonon energy (maximum phonon energy ~750 $cm^{-1}$, and borate ~1400 $cm^{-1}$, silicate ~1100 $cm^{-1}$ and phosphates ~1300 $cm^{-1}$), the high up-conversion efficiency and low melting temperature, high optical transmittance, high refractive index and so on [5–7]. Rare earth-doped oxyfluoride glass–ceramics has become one of the hot spot in optical materials research.

Since 1991, Komatsu et al. [8] had first prepared tellurite glass–ceramics containing nanocrystals, the oxyfluoride tellurite glass–ceramics has made great strides. Yu et al. [9], Pan et al. [10], Gang et al. [11] and Tatar et al. [12] prepared oxyfluoride tellurite glass–ceramics containing nanocrystals and studied their crystallization properties, thermal stability and optical properties. But oxyfluoride tellurite glass precursor generally contained $PbF_2$ or $CdF_2$ in order to widen the glass forming regions, which are harmful to environment and human. In addition, it is difficult for oxyfluoride tellurite glass–ceramics to reach high transparency, because tellurite glass devitrify easily. Consequently, oxyfluoride tellurite glass–ceramics without $PbF_2$, $CdF_2$ and $Pb_{1-x}Cd_xF_2$ nanocrystals have been less reported.

In this work, $Er^{3+}$-doped transparent oxyfluoride tellurite glass without Pb, Cd elements was prepared by melt-annealing, and transparent oxyfluoride tellurite glass–ceramics containing $CaF_2$ nanocrystals was obtained by subsequent controlled heat-treatment process. $Er^{3+}$-doped oxyfluoride tellurite glass–ceramics is a kind of ideal matrix materials in luminescence field.

## 2. Experimental

### 2.1. Preparation

Glass composition (mol%): 32$TeO_2$–15$SiO_2$–28$AlF_3$–15CaO–10NaF–1.5$ErF_3$, $TeO_2$ and $ErF_3$ are high-purity, NaF, $SiO_2$ and CaO are analytically pure. $AlF_3$ is chemical pure. The batch were fully mixed and then melted in a platinum crucible with a lid at 850 °C for 30 min in air, and then heated up to 1000 °C for homogenization and clarification in the silicon carbide rod electrical resistance heating furnace, the melt was poured on a stainless steel plate at 300 °C to shape, subsequently moved immediately to the furnace and annealed at 350 °C for 3 h to relieve internal stress, and then cooled down to the room temperature at the furnace. Finally, clear, transparent and bubble-free glass was obtained, marked A. The precursor glass and glass–ceramics samples were mechanically polished to a mirror finish with $CeO_2$ powders.

### 2.2. Characterization

Thermal property of the precursor glass was measured by differential scanning calorimeter (DSC, NETZSCH STA 409 C/CD, Germany) from room temperature to 850 °C at a heating rate of 10 °C/min, $N_2$ atmosphere. An X-ray powder diffraction system (D/max 2550HB+/PC, Rigaku, Japan) with CuKα radiation (0.154056 nm) was used for identification of the crystal phase, at 50 kV and 300 mA, the 2$\theta$ scanning range was 15°–85° at a rate of 4°/min. Field emission scanning electron microscope (S-4800FESEM, Hitachi, Japan) was used to study the glass–ceramics morphology, the grain size and distribution in the residual glass matrix. The network structure of glass and glass–ceramics were confirmed by Fourier infrared

* Corresponding author.
*E-mail addresses:* zhaoxiahou@sina.com, luckyxia2007@126.com (Z.-x. Hou).

0925-8388/$ – see front matter © 2011 Elsevier B.V. All rights reserved.
doi:10.1016/j.jallcom.2011.11.013

**Table 1**
Heat-treatment schedules and appearance.

| No. | Nucleation temperature/°C | Nucleation time/h | Crystallization temperature/°C | Crystallization time/h | Appearance |
|---|---|---|---|---|---|
| B | 370 | 4 | 420 | 6 | Transparent |
| C | 370 | 4 | 420 | 8 | Translucent |
| D | | | 430 | 10 | Opaque |

spectrometer (FT-IR, model IFS55, BRUKER, Germany) with resolution of 4 $cm^{-1}$ over the range of 4000–400 $cm^{-1}$ at room temperature. Transmittance of the precursor glass and glass–ceramics were measured by Uv–Vis scanning spectrophotometer (UVmini1240, Japan). The fluorescence spectra were obtained with an UV–Vis–IR spectrofluorimeter (Fluorolog-3, HORIBA-JOBINYVON, France) under the excitation of 980 nm LD. The InAs detector worked at liquid nitrogen temperature.

## 3. Results and discussion

### 3.1. Thermal property

The glass transition temperature $T_g$, crystallization initial temperature $T_x$ and crystallization peak temperature $T_c$ are determined 370 °C, 410 °C and 440 °C, respectively according to the DSC curve in Fig. 1. Various heat treatment processes are established and given in Table 1.

### 3.2. Crystal phase composition, microstructure and morphology

X-ray diffraction (XRD) patterns of oxyfluoride tellurite glass and glass–ceramics are shown in Fig. 2. It can be seen from Fig. 2 that there is only halo patterns without any sharp peaks are observed in curve A, it is confirmed that sample A is amorphous glass. Obvious crystallization peaks can be observed in B, C and D curves, all the peaks are analyzed with the standard sample spectra JSPDF (03-065-0535), the sole crystal phase $CaF_2$ is identified. It is noted that the intensity of $CaF_2$ crystal phase becomes larger with the increase of the heat-treatment temperature and time duration. However, the XRD peak positions of $CaF_2$ nanocrystals formed by the crystallization in precursor glass A shift towards lower diffraction angels compared with $CaF_2$ bulk crystals standard sample. According to the Bragg's law, diffraction angels shifting towards left indicates that interplanar crystal spacing increases. Considering the ionic radii, $r$, of $Ca^{2+}$ ($r$ = 0.100 nm) and $Er^{3+}$ ($r$ = 0.089 nm), and $Ca^{2+}$ ions are cubic close packing in $CaF_2$ unit cell, the lattice spacing should decrease if smaller $Er^{3+}$ ions replaced larger $Ca^{2+}$ ions, while the interplanar crystal spacing increases according to the results of XRD analysis, so the incorporation of $Er^{3+}$ ions into the octahedral interstice of $CaF_2$ nanocrystals is suggested.

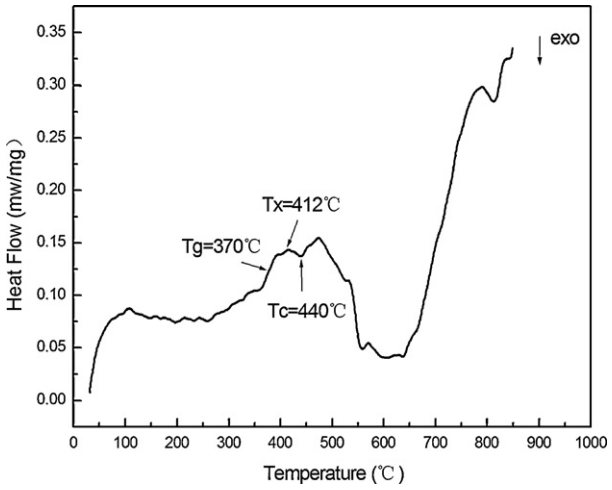


**Fig. 1.** DSC curve of the oxyfluoride tellurite precursor glass.

FESEM photograph of oxyfluoride tellurite glass–ceramics B is shown in Fig. 3. The spherical $CaF_2$ nanocrystals embed homogeneously among the glassy matrix after crystallization. The grain size of sample B is about 45 nm. Sample B is transparent, which could be proved by the transmittance curve in Section 3.4.

### 3.3. Glass and glass–ceramics network structure

Infrared absorption spectra of the transparent oxyfluoride tellurite glass and glass–ceramics are shown in Fig. 4. The strong absorption peaks can be seen at around 450 $cm^{-1}$, 560 $cm^{-1}$, 750 $cm^{-1}$, 1018 $cm^{-1}$, 1640 $cm^{-1}$ and 3440 $cm^{-1}$ in glass and glass–ceramics IR spectra.

Absorption peaks at 450 $cm^{-1}$ are contributed to the O–Si–O bonds bending vibration, absorption peaks at 570 $cm^{-1}$ are contributed to the Al–O–Al bonds bending vibration of [$AlO_6$]

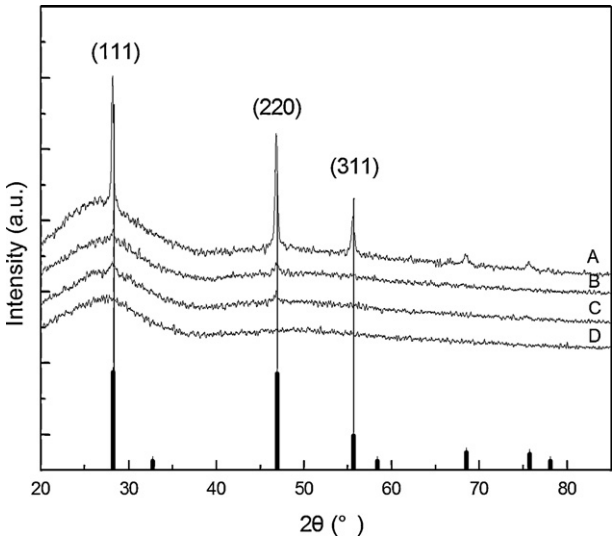


**Fig. 2.** XRD patterns of oxyfluoride tellurite precursor glass and glass–ceramics.

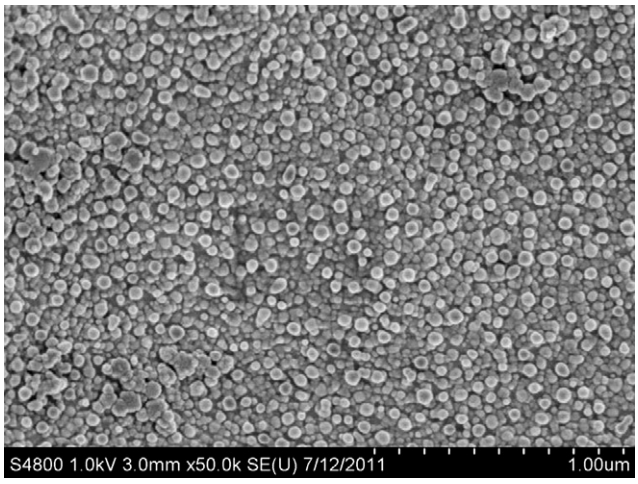


**Fig. 3.** FESEM photographs of glass–ceramics.

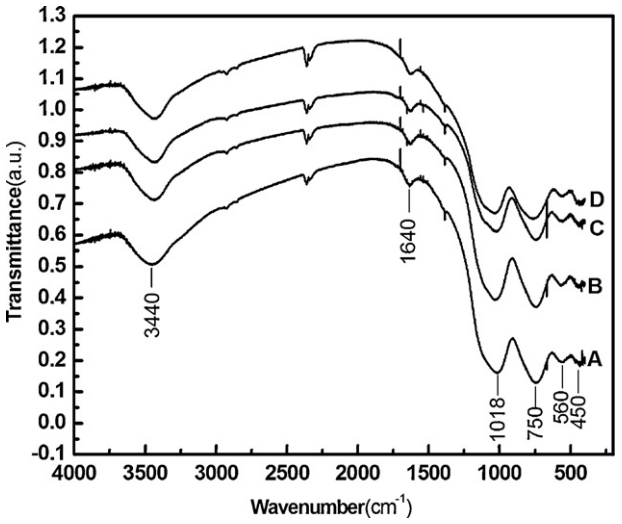


**Fig. 4.** Infrared spectra of oxyfluoride tellurite precursor glass and glass–ceramics.

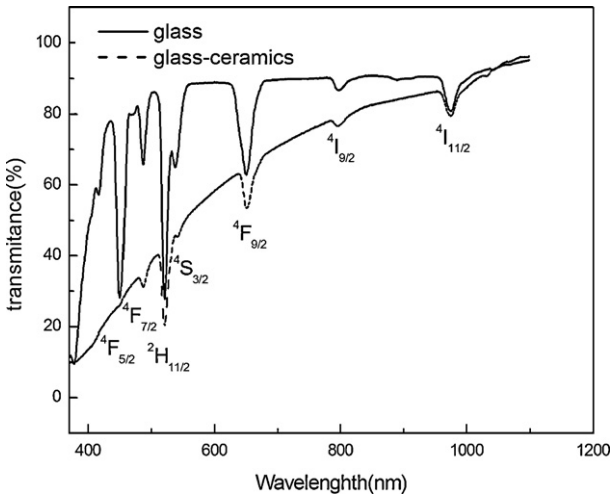


**Fig. 5.** Transmittance spectra of $Er^{3+}$-doped precursor glass and glass–ceramics.

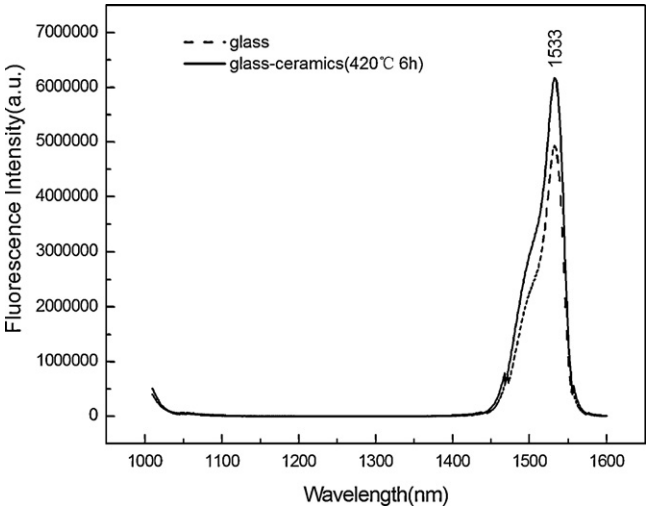


**Fig. 6.** Fluorescence spectra of $Er^{3+}$-doped precursor glass and glass–ceramics under 980 nm excitation.

octahedron. Absorption peaks at 750 $cm^{-1}$ are contributed to the stretching vibration of Te–O bonds in the [$TeO_3$] triangular pyramid structure. The introduction of fluorine in the oxyfluoride tellurite glass would make Te–O bonds fracture of O–Te–O in [$TeO_4$] double triangular pyramids, and convert to [$TeO_3$] triangular pyramids. The absorption peak at 620 $cm^{-1}$ is not obvious, which indicates that there is less [$TeO_4$] double triangular pyramid in glass matrix.

The absorption peaks at 1018 $cm^{-1}$ correspond to the Si–O–Al bond asymmetric stretching vibration, the atomic radii of Al and Si are similar, so Al atoms replace Si atoms to form [$AlO_4$] tetrahedron, Al atoms act as glass forming body to strengthen glass network structure.

Obvious infrared absorption peaks at 1640 $cm^{-1}$ and 3440 $cm^{-1}$ corresponds to the vibration of $H_2O$ and –OH groups. Absorption peaks of $H_2O$ and –OH groups are mainly due to crystal water contained in $AlF_3$ raw materials and without any atmosphere protection during melting.

Compared with the infrared absorption peaks of oxyfluoride tellurite glass, glass–ceramics has no remarkable difference, which indicates that the crystallization process has no markedly effect on the glass matrix network structure.

### 3.4. Glass and glass–ceramics transmittance

The transmittance spectra of $Er^{3+}$-doped precursor glass and transparent glass–ceramics B are shown in Fig. 5. The obvious absorption peaks can be seen at 975, 798, 652, 540, 520, 489 and 451 nm, corresponding to the transitions from the ground state $^4I_{15/2}$ to the excited states $^4I_{11/2}$, $^4I_{9/2}$, $^4F_{9/2}$, $^4S_{3/2}$, $^2H_{11/2}$, $^4F_{7/2}$ and $^4F_{5/2}$ of $Er^{3+}$ ions, respectively. The transmittance of glass–ceramics can reach 78% at 780 nm and 90% at 1017 nm.

### 3.5. Glass and glass–ceramics fluorescence spectra

Fig. 6 shows the fluorescence spectra of precursor glass and transparent glass–ceramics B in the range of 1000–1600 nm. The broad emission band of the $Er^{3+}$ ions corresponds to the $^4I_{13/2} \rightarrow {}^4I_{15/2}$ transition at 1533 nm. The FWHM (full width at half maximum) of this emission band increases from 39.16 nm to 43.37 nm after crystallization. And the relative fluorescence intensity at 1553 nm increases obviously as well. $Er^{3+}$ ions in the oxyfluoride glass are mainly coupled to the non-bridging oxygen on the O–Te and/or O–Si (Al) bonds with relatively high phonon energies, while in oxyfluoride glass–ceramics $Er^{3+}$ ions are incorporated into $CaF_2$ nanocrystals with low phonon energies.

## 4. Conclusions

$Er^{3+}$-doped oxyfluoride tellurite glass $32TeO_2$–$15SiO_2$–$28AlF_3$–$15CaO$–$10NaF$ was prepared successfully, and the transparent oxyfluoride glass–ceramics containing $CaF_2$ nanocrystals was obtained by controlled heat-treatment at 370 °C nucleation for 4 h and at 420 °C crystallization for 6 h. $CaF_2$ nanocrystals sized at 45 nm are spherical and embed homogeneously among the glassy matrix. Te and Si atoms exist in [$TeO_3$] and [$SiO_4$] forms. Part of Al atoms exists in the forms of [$AlO_4$] and form network together with [$SiO_4$] tetrahedron. The other Al atoms exist in the forms of [$AlO_6$] as modifiers. The transmittance of glass–ceramics can reach 78% at 780 nm and 90% at 1017 nm. The broad emission band of the $Er^{3+}$ ions corresponds to the $^4I_{13/2} \rightarrow {}^4I_{15/2}$ transition at 1533 nm. The FWHM of this emission band increases from 39.16 nm to 43.37 nm after crystallization. $Er^{3+}$ ions are incorporated into $CaF_2$ nanocrystals with low phonon energies.

## Acknowledgements

Thanks for the financing by the Department of Science and Technology in Liaoning province of China – Nature Science Foundation (no. 20102156), the Department of Education of Liaoning province – University Scientific Research Program (no. L2010371), the Department of Science and Technology in Shenyang city of China – Science and Technology Program (no. 1091178-1-00) and the Department of Science and Technology in Shenyang city of China – Key Laboratory Construction Project (no. F10216100).

## References

[1] S.F. León-Luis, J. Abreu-Afonso, J. Pena-Martínez, et al., J. Alloys Compd. 479 (2009) 557.
[2] R. Santos, L.F. Santos, R.M. Almeida, J. Non-Cryst. Solids 356 (2010) 2677.
[3] D.Q. Chen, Y.S. Wang, Y.L. Yu, et al., J. Solid State Chem. 179 (2006) 1445.
[4] I. Jlassi, H. Elhouichet, M. Ferid, et al., Opt. Mater. 32 (2010) 743.
[5] N. Jaba, H.B. Mansour, B. Champagnon, Opt. Mater. 31 (2009) 1242.
[6] J.J. Zhang, Z.C. Duan, D.B. He, et al., Laser Optoelectron. Progress 42 (2005) 2.
[7] G. Upender, C.P. Vardhani, S. Suresh, et al., Mater. Chem. Phys. 121 (2010) 335.
[8] T. Komatsu, H. Tawarayama, H. Mohri, et al., J. Non-Cryst. Solids 135 (1991) 105.
[9] C.L. Yu, D.B. He, G.N. Wang, et al., China Opt. Lett. 8 (2010) 197.
[10] Z. Pan, A. Ueda, R. Mu, et al., J. Lumin. 126 (2007) 251.
[11] G. Zhou, S.X. Dai, C.L. Yu, et al., J. Chinese Rare Earth 23 (2005) 519.
[12] D. Tatar, M.L. Ovecoglu, G. Özen, et al., J. Eur. Ceram. Soc. 29 (2009) 329.